Supporting information

Modification of mixed-nitrogen anions configuration for accelerate lithium ions transport on the $LiFePO_4$ electrode

Jin-young Choi[a], Hye-min Kim[*b], Yu-sung Kim[a], In-sik Lee[a], Byung-chul Cha[b] and Dae-wook Kim[*a]

a) Advanced Manufacturing Process R&D Group, Ulsan Regional Division, Korea Institute of Industrial Technology (KITECH), 55, Jongga-ro, Jung-gu, Ulsan, 44313, Korea

b) Department of Materials Chemistry, Shinshu University, 4-17-1, Wakasato, Nagano, 3808553, Japan

*Corresponding to Author: dwkim@kitech.re.kr, hmkim545@gmail.com

Table. S1 Details of PIII process conditions.

Sample	Plasma generation conditions			Ion implantation conditions			
	Process pressure (torr)	RF power (W)	N_2 gas flow (sccm)	Implantation energy (kV)	Pulse width (μs)	Frequency (Hz)	Implantation time (s)
LFP-N5	2.0×10^{-3}	300	30	5	3.0	500	60
LFP-N7				7			

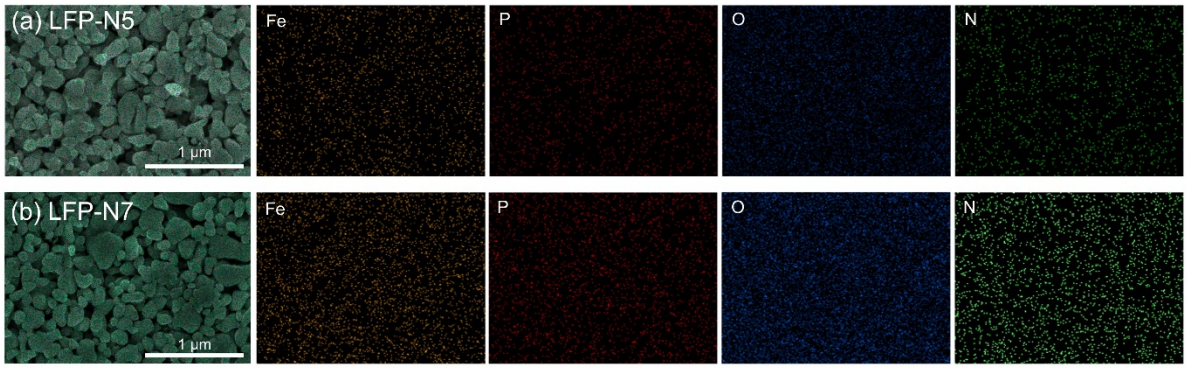

Fig. S1 FE-SEM EDS mapping images for Fe, P, O and N of (a) LFP-N5 and (b) LFP-N7.

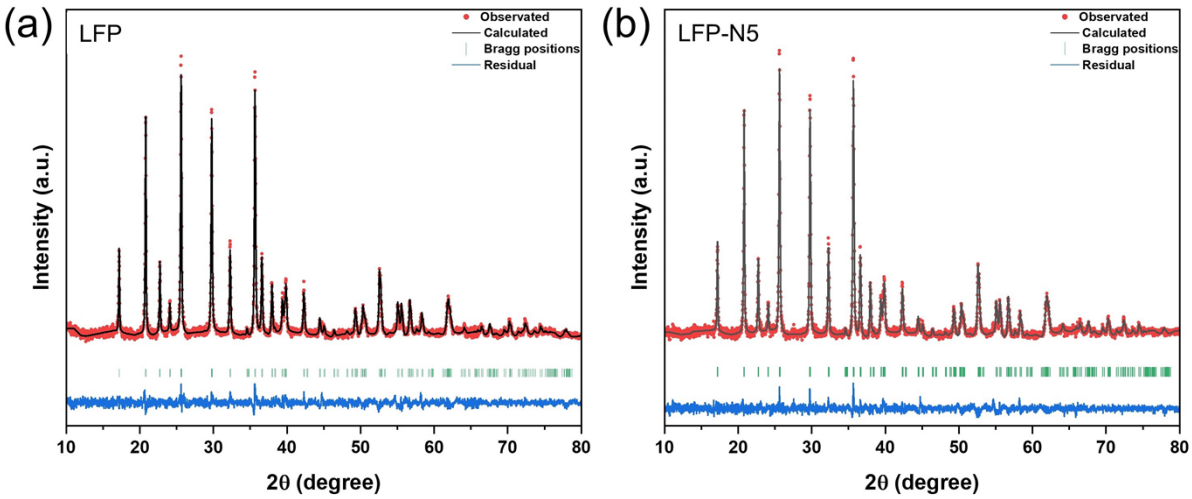

Fig. S2 Rietveld refinement patterns of (a) LFP and (b) LFP-N5.

Table S2. Cell parameters of LFP, LFP-N5 and LFP-N7 obtained from Rietveld refinement of XRD.

	Cell parameter								
	a	b	c	volume (Å)	σ	β	γ	R_p	R_{wp}
LFP	10.3176	6.0017	4.692	290.542	90	90	90	5.38	8.37
LFP-N5	10.3167	6.0009	4.6893	290.314	90	90	90	5.32	8.11
LFP-N7	10.3124	5.9973	4.6863	289.829	90	90	90	5.87	8.52

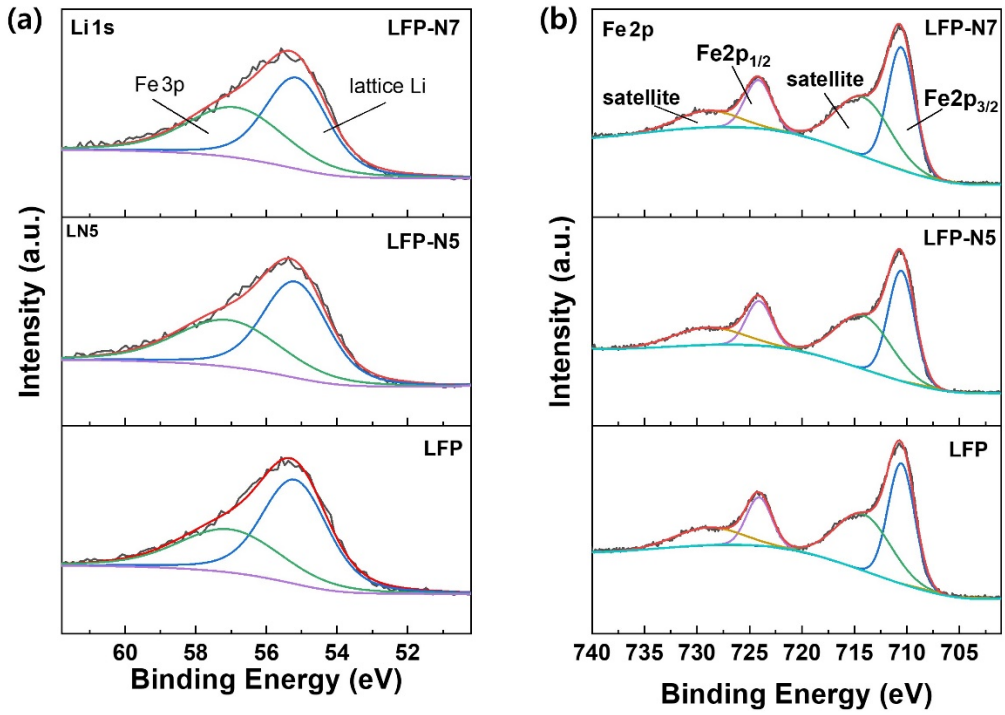

Fig. S3 Li 1s and Fe 2p XPS core-level spectra of LFP, LFP-N5 and LFP-N7.

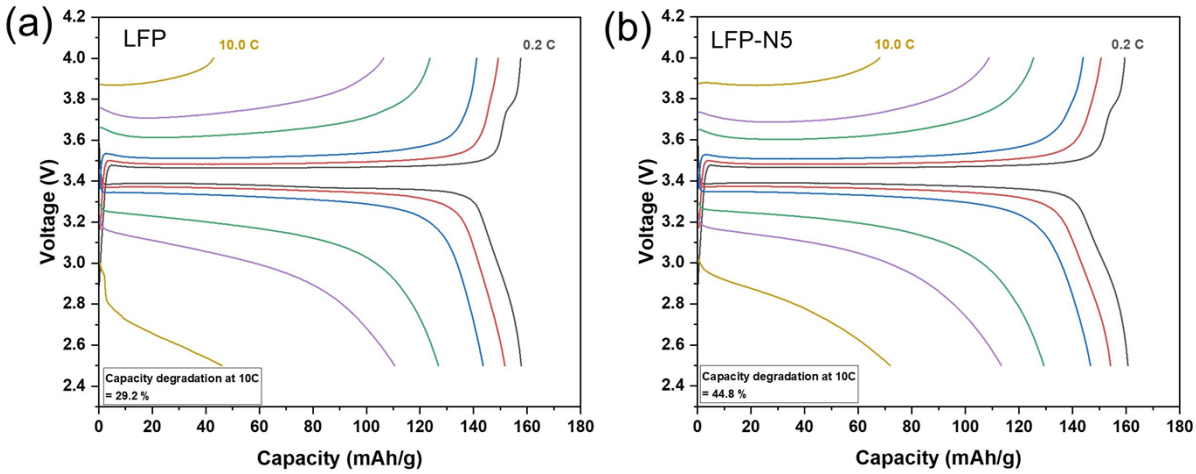

Fig. S4 Galvanostatic charge-discharge curves of LFP and LFP-N5 at varies C-rate.

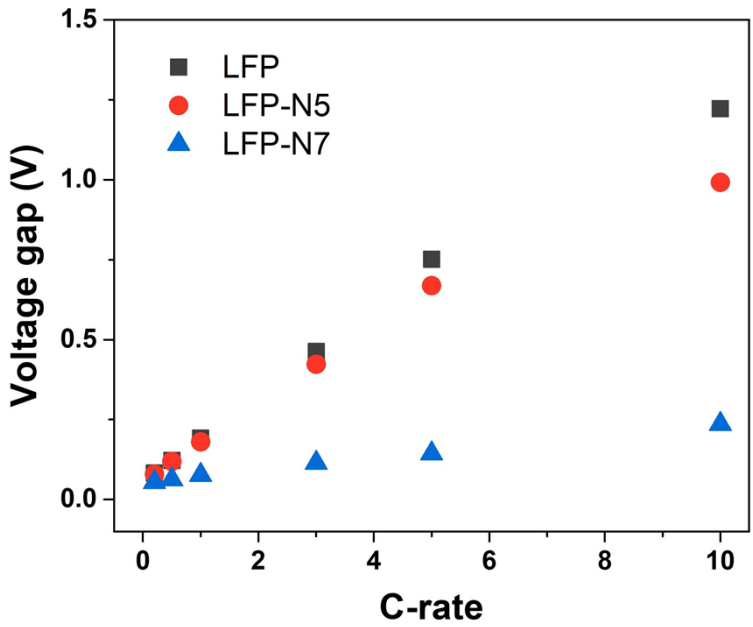

Fig. S5 Relationship between the C-rate and voltage gap of the charge/discharge voltage plateau.

Table S3. EIS kinetic parameters of LFP, LFP-N5 and LFP-N7 electrode.

	R_{sf} (ohm)	R_{ct} (ohm)	D_{Li} (cm^2 s^{-1})
LFP	3.34	123.1	3.74×10^{-14}
LFP-N5	3.57	104.6	5.43×10^{-14}
LFP-N7	4.19	31.5	3.46×10^{-13}

Table S4 Rate performance of anion surface modification of LFP.

Sample	Method	Performance	Ref.
Cl-doped $LiFePO_4$/C	solid-state reaction	105.3 mAh g^{-1} @ 10C	[1]
$LiFe(PO_4)_{0.9}F_{0.3}$/C	co-precipitation reaction followed by high-temperature treatment	110 mAhg g^{-1} @ 10C	[2]
$LiFePO_{3.938}F_{0.062}$/C	solid-state reaction	102.3 mAh g^{-1} @ 10C	[3]
S-doped $LiFePO_4$	solvothermal method	112.7 mAhg g^{-1} @ 10C	[4]
F-doped $LiFePO_4$@N/B/F-doped carbon	hydrothermal method	116.4 mAh g^{-1} @ 5 C 71.3 mAh g^{-1} @15C	[5]
Cl-doped $LiFePO_4$/C	carbothermal reduction route	110 mAh g^{-1} @ 10C	[6]
$LiFePO_xN_y$ thin films	Reactive magnetron sputter deposition	100 mAh g^{-1} @ 10C	[7]
S-doped $LiFePO_4$ @N/S-doped C	solvothermal method	121.26 mAh g^{-1} @ 5 C	[8]
$Li_{0.94}FePO_{3.84}N_{0.16}$	sol–gel approaches- thermal nitridation	~60 mAh g^{-1} @ 5 C	[9]
LFP-N7	plasma-immersion ion implantation (PIII)	128 mAhg g^{-1} @10C	This work

References

1. H. Liu, S.-h. Luo, S.-x. Yan, Y.-f. Wang, Q. Wang, M.-q. Li and Y.-h. Zhang, J. Electroanal. Chem., 2019, 850, 113434.
2. C. Gao, J. Zhou, G. Liu and L. Wang, J. Alloys Compd., 2017, 727, 501-513.
3. Z. Yan, D. Huang, X. Fan, F. Zheng, Q. Pan, Z. Ma, H. Wang, Y. Huang and Q. Li, Front. Mater., 2020, 6, 341.
4. K. Okada, I. Kimura and K. Machida, RSC Adv., 2018, 8, 5848-5853.
5. Y. Meng, Y. Li, J. Xia, Q. Hu, X. Ke, G. Ren and F. Zhu, Appl. Surf. Sci., 2019, 476, 761-768.
6. C. Sun, Y. Zhang, X. Zhang and Z. Zhou, J. Power Sources, 2010, 195, 3680-3683.
7. K.-F. Chiu, S.-H. Su, H.-J. Leu and Y. R. Jheng, ECS Trans., 2016, 73, 27.
8. B. Zhang, S. Wang, L. Liu, J. Wang, W. Liu and J. Yang, Nanotechnology, 2022, 33, 405601.
9. S. F. Mayer, C. de la Calle, M. T. Fernández-Díaz, J. M. Amarilla and J. A. Alonso, RSC Adv., 2022, 12, 3696-3707.